

Continuous parameter working memory in a balanced chaotic neural network

Nimrod Shaham¹ and Yoram Burak^{1,2}

¹*Racah Institute of Physics, The Hebrew University of Jerusalem*

²*Edmond and Lily Safra Center for Brain Sciences, The Hebrew University of Jerusalem*

(Dated: December 14, 2018)

Working memory, the ability to maintain information over time scales greater than those characterizing single neurons, is essential to many brain functions. It remains unclear whether neural networks in the balanced state, an important model for activity in the cortex, can support a continuum of stable states that would make it possible to store a continuous variable in working memory while also accounting for the stochastic behavior of single neurons. Here we propose a simple neural architecture that achieves this goal. We show analytically that in the limit of an infinite network a continuous parameter can be stored indefinitely on a continuum of balanced states. For finite networks we calculate the diffusivity along the attractor driven by the chaotic noise in the network, and show that it is inversely proportional to the system size. Thus, for large enough (but realistic) neural population sizes, and with suitable tuning of the network connections, it is possible to maintain continuous parameter values over time scales larger by several orders of magnitude than the single neuron time scale.

The brain is able to perform tasks that demand precision while using highly fluctuating and noisy hardware. The irregular dynamics observed in neuronal activity are often modeled as arising from noisy inputs or from intrinsic noise in the dynamics of single neurons. However, theoretical and experimental works have suggested that explanations based on sources of noise in intrinsic neural dynamics are insufficient to account for the stochastic nature of activity in the cortex [1–3]. An alternative proposal is that noise in the cortex arises primarily from chaotic dynamics at the network level. In neural networks in the balanced state [3, 4], chaotic activity induces apparent stochasticity in the activity of single units, despite the absence of intrinsic random noise. Thus, the theory of balanced neural networks provides a compelling explanation for the stochastic nature of cortical activity.

It remains unclear which computational functions in the brain are compatible with the architecture of the balanced network model, since this model assumes random, unstructured connectivity in its rudimentary form. The possibility that functional circuits in the brain are in a balanced state raises another important question: does the apparent stochasticity of single neurons in the balanced state have similar consequences on function as would arise from stochasticity which is truly intrinsic to the dynamics of individual neurons and synapses?

Here we explored the effects of chaotic noise on continuous parameter working memory, a task which is particularly sensitive to noise. Attractor dynamics [5] are often put forward as a mechanism for the persistent neural activity underlying this task. The dynamics of continuous attractor networks are characterized by a continuum of marginally stable steady states which make it possible to memorize parameters with a continuous range of values [5–9].

In continuous attractor networks, noise can cause diffusion along the manifold of steady states, leading to degra-

dation of the stored memory [10–13]. Previous studies of stochastic effects on continuous attractor dynamics assumed intrinsic random noise in the neuronal activity or in the input, or in both. For this reason we examined whether a balanced network can be constructed with a continuum of marginally stable states, and how, in this scenario, chaotic noise would affect the maintenance of the stored memory.

The broader question of whether balanced networks can produce persistent activity has attracted considerable theoretical interest in recent years. Several works have used a mechanism of clustered connections to obtain slow dynamics [14–16]. Others have used short term synaptic plasticity [17, 18], or different synaptic time scales to generate slow dynamics through a derivative feedback mechanism [19, 20]. However, previous works have not demonstrated the existence of a continuum of steady states in a balanced neural network analytically, and it remains unclear whether such a continuum can be obtained without evoking additional mechanisms, such as short-term synaptic plasticity or derivative feedback.

Here we identify an architecture in which slow dynamics are attainable in a simple form of a balanced network. Using a mean field approach, we prove the existence of a continuum of balanced states in our model in the large population limit. In finite networks we show that the chaotic noise drives diffusive motion along the attractor. We calculate the diffusivity and show that it scales inversely with the system size, as predicted for continuous attractor networks with intrinsic sources of neuronal stochasticity. For a reasonable number of neurons and suitable tuning, our network can operate as a working memory network.

Our neural network model is based on the classical balanced network model presented in Refs. [3, 4]. This model consists of two distinct populations, one inhibitory and the other excitatory. The recurrent connectivity is

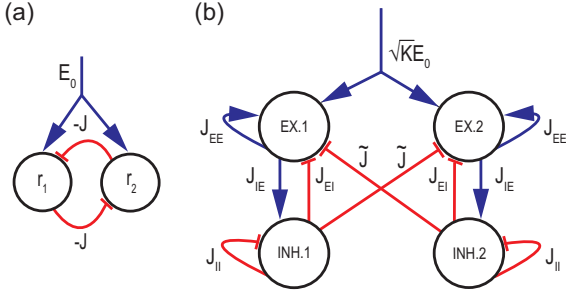


FIG. 1. (a) Two neural populations with rates r_1, r_2 inhibit each other with synaptic efficacies $-J$. (b) Two coupled balanced subnetworks, each consisting of an excitatory and inhibitory population of N neurons. Connections within each network are random with a connection probability K/N , $1 \ll K \ll N$. Connection strengths are: J_{EE}/\sqrt{K} , J_{IE}/\sqrt{K} , J_{EI}/\sqrt{K} and J_{II}/\sqrt{K} according to the identity of the participating neurons. Without loss of generality, we chose $J_{EE} = J_{IE} = 1$ and defined $J_{EI} \equiv -J_E$, $J_{II} \equiv -J_I$. Mutual inhibition is generated by all-to-all connections of strength $-\tilde{J}\sqrt{K}/N$ from each inhibitory population to the excitatory population of the other subnetwork. An excitatory input $\sqrt{K}E_0$ is fed into both excitatory populations.

random with a probability K/N for a connection, where N is the population size (assumed for simplicity to be the same in both populations), K is the average number of connections per neuron from each population, and the connection strength is $\sim 1/\sqrt{K}$. The neuron activity (0 or 1) is determined in each update by the sign of the total input to the neuron minus a threshold. For $1 \ll K \ll N$ and over a wide range of parameters, the mean population activity settles to a fixed point (the *balanced state*) where on average the total excitation received by each neuron is approximately canceled by the total inhibition. The single neuron activity appears noisy, neither of the populations is fully activated or deactivated, and the overall network state is chaotic.

Despite the nonlinearities involved in the dynamics of each neuron, the population averaged activities in the balanced state are linear functions of the external input [3, 4]. We exploit this linearity to build a simple system of two balanced networks projecting to each other. The intuition comes from a simple model of a continuous attractor neural network consisting of linear neurons arranged in two populations that mutually inhibit each other, Fig. 1(a). The linear rate dynamics of this system are given by:

$$\tau \dot{\mathbf{r}} = -\mathbf{r} + \mathbf{W}\mathbf{r} + \mathbf{E}, \quad (1)$$

where $\mathbf{E} = [E_0, E_0]$, $E_0 > 0$ is an external input and

$$\mathbf{W} = \begin{pmatrix} 0 & -J \\ -J & 0 \end{pmatrix}. \quad (2)$$

For $J = 1$ the system has a vanishing eigenvalue, and the fixed points form a continuous line: $r_1 + r_2 = E_0$.

In our model, a balanced subnetwork replaces each of these populations, and the inhibitory population in each network projects to the excitatory population of the other network, Fig. 1(b). As in [3, 4], the neurons are binary and are updated asynchronously, at update times that follow Poisson statistics. The mean time interval between updates is τ_E (τ_I) for neurons in the excitatory (inhibitory) populations. In each update of a neuron k from population i , the new state of the neuron σ_i^k is determined based on the total weighted input to the neuron,

$$\sigma_i^k = \Theta(u_i^k), \quad (3)$$

where Θ is the Heaviside step function, and u_i^k is the total input to the unit at that time,

$$u_i^k = \sum_{l=1}^4 \left[\sum_{j=1}^{N_l} J_{kl}^{ij} \sigma_j^l(t) + \sqrt{K} E_0^l \right] - T_k. \quad (4)$$

Here, T_k is the threshold and E_0 is an external input. We chose the external input to be zero for the inhibitory populations and to be positive (and constant) for the excitatory populations. We denote by u_i the mean of u_i^k over all the neurons k within the population i , and over the quenched noise. Similarly, we denote the variance of u_i^k by α_i . Similar to the case of a single balanced network [4], the mean field dynamics of the population averaged activities for $N \rightarrow \infty$ and $K \gg 1$ are given by:

$$\tau_i \dot{m}_i = -m_i + H(-u_i/\sqrt{\alpha_i}), \quad (5)$$

where $m_i(t) = 1/N \sum_{k=1}^N \sigma_i^k(t)$ [$i = 1$ (2) for the excitatory (inhibitory) population of the first subnetwork, and similarly $i = 3, 4$ in the second subnetwork] and $H(x)$ is the complementary error function. We chose the mutual inhibition between the subnetworks to be all to all, and scaled the interaction strength such that the total input to each neuron scaled with \sqrt{K} .

To check whether there exist parameters for which the system has a continuum of balanced states, it is convenient to write the steady state equations of the above dynamics as follows:

$$\begin{aligned} m_1 - J_E m_2 - \tilde{J} m_4 + E &= \frac{1}{\sqrt{K}} (T_1 - \sqrt{\alpha_1} H^{-1}(m_1)), \\ m_1 - J_I m_2 &= \frac{1}{\sqrt{K}} (T_2 - \sqrt{\alpha_2} H^{-1}(m_2)), \\ m_3 - J_E m_4 - \tilde{J} m_2 + E &= \frac{1}{\sqrt{K}} (T_3 - \sqrt{\alpha_3} H^{-1}(m_3)), \\ m_3 - J_I m_4 &= \frac{1}{\sqrt{K}} (T_4 - \sqrt{\alpha_4} H^{-1}(m_4)). \end{aligned} \quad (6)$$

Taking the limit $K \rightarrow \infty$ while requiring that none of the populations is fully on or off produces a linear system of equations for the mean activities. By choosing the interaction strength between the two subnetworks to be $\tilde{J} = J_E - J_I$, this system becomes singular, and has a continuum of solutions which are a continuum of stable balanced states. Note that in order to have mutual inhibition, \tilde{J} should be positive, or $J_E > J_I$ [21].

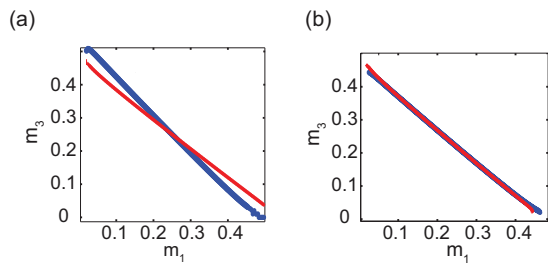


FIG. 2. (a) Nullclines in the $m_1 - m_3$ plane. $K = 1000$, $J_E = 4$, $J_I = 2.5$, $\tilde{J} = 1.5$, $\tau_E = 1$, $\tau_I = 0.8$, $E_0 = 0.3$. These values are used throughout the manuscript. (b) Same as (a), except that here \tilde{J} is tuned to ≈ 1.7 to achieve a singular Jacobian at the symmetric point.

In the limit of infinite N and finite (but large) K , the dynamics are still deterministic and described by Eq. (5). Eqs. (6) are now nonlinear, and a continuum of steady states cannot be established. However, if the nonlinear nullclines are close to each other, slow dynamics are attainable in a specific direction of the mean activity space. Note that there always exists a symmetric fixed point where $m_1 = m_3$ and $m_2 = m_4$. If in addition, at the symmetric point, the slopes of the nullclines are identical ($\partial m_3 / \partial m_1 = -1$), there is a vanishing eigenvalue for the mean field dynamics, Eq. (5), at this point (SM). Under these conditions, the eigenvalue is also expected to be small in the vicinity of the symmetric point. In fact, even for moderately large values of K , the two nullclines nearly overlap over a large range of m_1 and m_3 , Fig. 2(b) ($K = 1000$). By requiring the existence of a vanishing eigenvalue in the linearized dynamics around the fixed point, it is possible to obtain a nonlinear equation for \tilde{J} , which we solve numerically. In the limit of $K \rightarrow \infty$, the solution \tilde{J} approaches $J_E - J_I$.

The stability of the approximate line attractor can be probed by numerically evaluating the eigenvalues of the linearized dynamics along the line. For a large range of parameters, we obtain three large negative eigenvalues, and one eigenvalue which is negative but small (compared to τ_i^{-1}). Thus, the approximate line attractor is stable. An illustration of the existence of a direction in mean activity space, along which the dynamics are slow, is shown in Fig. S4.

We next consider the realistic case where both N and K are finite, while still requiring $N \gg K \gg 1$. We performed numerical simulations of networks with N ranging between 10^4 to 12×10^4 . To simplify the analysis, we chose the random weights within each subnetwork such that they precisely mirrored each other. This choice ensured that the fixed point would be symmetric ($m_1 = m_3$ and $m_2 = m_4$). When the connections in each subnetwork are chosen independently, the fixed point deviates slightly from this symmetry plane (this deviation approaches zero for infinite networks). All the results

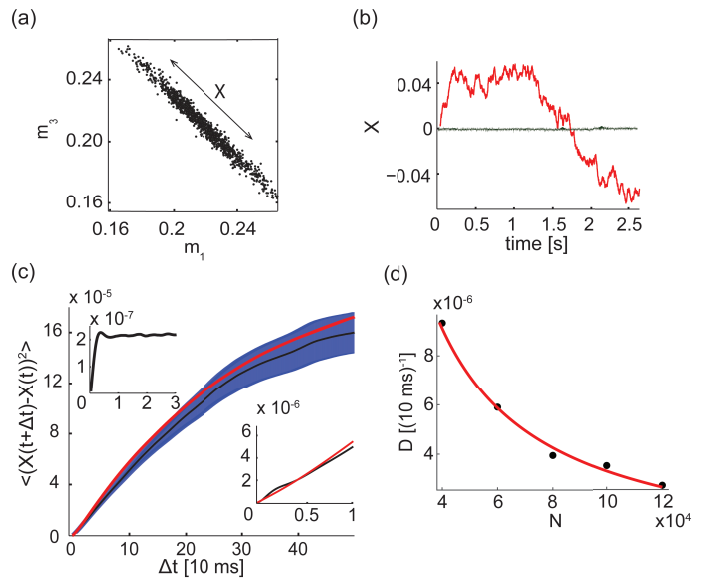


FIG. 3. (a) Projection of the mean activities on the $m_1 - m_3$ plane, for finite $N = 10^5$. (b) Dynamics of the projection along the special direction (red) and a perpendicular projection (black). (c) Measurements of $G(X, \Delta t)$ from simulations (black. Blue: standard deviation of the mean), compared with the semi-analytical approximation (Eq. (S28)) ($N = 1.2 \cdot 10^5$). Lower inset: zoom-in on $\Delta t \leq \tau$. Upper inset: similar measurements from a single, disconnected balanced network. (d) Diffusion coefficient as a function of N . Symbols: simulation results. Red: fit to $\sim 1/N$ dependence.

described below remain qualitatively valid.

In our simulation, individual neurons approximately exhibited exponential ISI distributions similar to those observed in the two population case, although their dynamics are deterministic. Fig. 3(a) shows the averaged population activity projected on the $m_1 - m_3$ plane. Fig. 3(b) shows the projection along the slow direction: $X(t) \equiv \mathbf{v}_0^T \cdot [\mathbf{m}(t) - \mathbf{m}_0]$, where \mathbf{m}_0 is the vector of mean population activities at the symmetric fixed point, and \mathbf{v}_0 is the left eigenvector of the linearized dynamics with an eigenvalue close to zero. Note that $X(t)$ exhibits slow diffusive dynamics, characterized by a timescale of ~ 1 s. To demonstrate that the dynamics are effectively one dimensional, a projection on a perpendicular direction is shown as well.

The dynamics of the projection X can be characterized as a stochastic process with the moments:

$$F(X, \Delta t) \equiv \frac{\langle X(t + \Delta t) - X(t) | X(t) = X \rangle_t}{\Delta t}, \quad (7)$$

$$G(X, \Delta t) \equiv \left\langle [X(t + \Delta t) - X(t)]^2 \middle| X(t) = X \right\rangle_t. \quad (8)$$

Eq. (7) characterizes the systematic drift along the attractor. For small Δt and near the fixed point, we expect $F(X, \Delta t) \approx -\lambda X$ with constant λ , characterizing

the timescale of decay towards the fixed point. In fact, we found that this relation held to a very good approximation over a wide range of positions along the approximate attractor (Fig. S2). In simulations of the finite N network, we estimated λ from measurements of $F(X, \Delta t)$ near the symmetric point, and tuned \bar{J} to obtain $\lambda^{-1} \gg \tau$. In Fig. 3, $\lambda^{-1} \simeq 3$ s.

Eq. (8) characterizes the random diffusion along the approximate line attractor, driven by the chaotic noise. Fig. 3(c) shows measurements of this quantity from simulations, for X near the symmetric fixed point. On short time scales compared to τ , G can be analytically approximated using the averaged autocorrelation function, $q_j(t) \equiv 1/N \sum_{i=1}^N \langle \sigma_i^j(t + \Delta t) \sigma_i^j(t) \rangle$. Using an expression for q , derived in Ref. [4] for a network with a single fixed point, we obtain, for $\Delta t \lesssim \tau$,

$$G(X, \Delta t) \approx \frac{2\Delta t}{N} \sum_{j=1}^4 (v_j^0)^2 \left[-\frac{\partial q_j(t)}{\partial t} \right] \Big|_{t \rightarrow 0}, \quad (9)$$

where v^0 is the left eigenvector of the system's Jacobian with an eigenvalue close to zero (SM). Note that G is proportional to Δt and inversely proportional to N .

A similar scaling of $G(X, \Delta t)$ with N and Δt also holds in the single balanced network in Ref. [4], for $\Delta t \ll \tau$. However, in the case of a single balanced network, G saturates for $\Delta t \gtrsim \tau$ (upper inset in Fig. 3(c)). On time scales larger than τ , the behavior of our network differs dramatically from that of the single balanced network, since G continues to increase as a function of Δt , up to Δt of order λ^{-1} (Fig. 3(c)). Thus, the diffusive motion generates correlated activity over time scales much longer than τ . Because the chaotic noise is uncorrelated on time scales larger than τ , and since λ is approximately constant along the attractor, we expect the motion to approximately follow the statistics of an Ornstein-Uhlenbeck (OU) process. This approximation provides a good fit to the dynamics, Figs. S3 and 4(b), as expected. This made it possible to extract a diffusion coefficient D from the simulations which characterizes the random motion on time scales $\tau \lesssim \Delta t \lesssim \lambda^{-1}$.

According to Eq. (9), fluctuations in the mean activity scale as $1/N$, but this equation is valid only for time scales smaller than τ , whereas the diffusion coefficient D characterizes fluctuations on longer time scales. Figure 3(d) demonstrates that the diffusion coefficient, extracted from a fit to the statistics of an OU process, is inversely proportional to N . The same scaling with N is observed in continuous attractor networks with intrinsic neural stochasticity [10].

To understand this result in more detail, we start by considering the time dependent correlation functions of m_i in a single balanced network. An analytical expression for these correlation functions is not available (see [22] for further discussion), but our simulations show that they decay over time scales of order τ , and that they scale

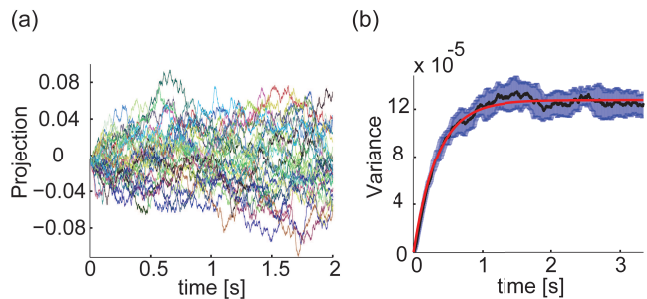


FIG. 4. Chaotic nature of the noise driving the diffusive motion. (a) Projections of the mean activities over the special direction in 30 trials with the same update schedule and the same initial conditions, except for one neuron which was flipped in each population ($N = 10^5$). (b) Variance over 1500 trials as a function of time, with 2σ errorbars. Red: fit to the variance of an OU process ($D \simeq 3.4 \cdot 10^{-6} 1/10$ s).

as $1/N$, Fig. S5. Furthermore, we showed (SM) that the statistics of diffusion in the coupled system can be expressed precisely in terms of the correlation functions of the single, uncoupled balanced networks (Eq. S24). The measurements of G from simulations are in excellent agreement with this analytical prediction, Fig. 3(c). Thus, the correlation structure of the chaotic noise in the single balanced network determines the statistics of diffusive motion along the attractor in the coupled two-population network. The $1/N$ scaling of the diffusion coefficient (Fig. 3(d)) is a consequence of the decay with N of cross correlations in activity of different neurons in the single balanced network: in this sense, for large N the network behaves as a collection of neurons with independent random noise.

Finally, we briefly address the chaotic nature of the noise that drives diffusive motion. Figure 4(a) shows results from multiple simulations in which the initial network state differed solely by a flip of one neuron in each population (out of $\sim 10^5$ neurons). All other parameters, including the asynchronous update schedule and the network weights were identical across runs. The time dependence of the variance across different runs was similar to the variance over realizations of an OU process, Fig. 4(b), with a similar diffusion coefficient as observed in the fit for $G(X, \Delta t)$ [Fig. 3(c)]. Thus, the different initial conditions are equivalent to different realizations of dynamic noise that drives diffusive motion along the approximate line attractor.

In summary, we demonstrated that slow dynamics along a continuous line in the population mean activity space are attainable in a simple balanced network. In finite networks, the chaotic dynamics of neural activity drive diffusive motion along the attractor. We calculated the diffusivity in the system, based on the correlation structure observed in a single balanced network, and showed that the diffusion coefficient along the attractor is

inversely proportional to the network size. This is similar to the effect of noise that arises from intrinsic neural or synaptic mechanisms [10]. Thus, the persistence of the network can be improved by increasing the number of neurons. In a network with 10^5 neurons per population, diffusion over one second causes a deflection of $\sim 10^{-2}$ in units of mean activity, compared to a range of order unity. This network size is sufficient, with proper tuning of the synaptic weights, to achieve persistence times of several seconds, which is much greater than the single neuron time scale.

We thank Sophie Deneve for the helpful discussion, and Haim Sompolinsky for comments on the manuscript. This research was supported by the Israel Science Foundation grant No. 1733/13 and (in part) by grant No. 1978/13. We acknowledge support from the Gatsby Charitable Foundation, and from the Rudin Foundation (NS).

-
- [1] Z. F. Mainen and T. J. Sejnowski, "Reliability of spike timing in neocortical neurons," *Science*, vol. 268, no. 5216, pp. 1503–1506, 1995.
- [2] G. R. Holt, W. R. Softky, C. Koch, and R. J. Douglas, "Comparison of discharge variability in vitro and in vivo in cat visual cortex neurons," *Journal of Neurophysiology*, vol. 75, no. 5, pp. 1806–1814, 1996.
- [3] C. van Vreeswijk and H. Sompolinsky, "Chaos in neuronal networks with balanced excitatory and inhibitory activity," *Science*, vol. 274, no. 5293, pp. 1724–1726, 1996.
- [4] C. van Vreeswijk and H. Sompolinsky, "Chaotic balanced state in a model of cortical circuits," *Neural computation*, vol. 10, pp. 1321–1371, Aug. 1998. PMID: 9698348.
- [5] H. S. Seung, "How the brain keeps the eyes still," *Proceedings of the National Academy of Sciences*, vol. 93, pp. 13339–13344, Nov. 1996. PMID: 8917592.
- [6] D. A. Robinson, "Integrating with neurons," *Annual Review of Neuroscience*, vol. 12, no. 1, pp. 33–45, 1989. PMID: 2648952.
- [7] A. Compte, N. Brunel, P. S. Goldman-Rakic, and X.-J. Wang, "Synaptic mechanisms and network dynamics underlying spatial working memory in a cortical network model," *Cerebral Cortex*, vol. 10, no. 9, pp. 910–923, 2000.
- [8] O. Barak, D. Sussillo, R. Romo, M. Tsodyks, and L. Abbott, "From fixed points to chaos: three models of delayed discrimination," *Progress in neurobiology*, vol. 103, pp. 214–222, 2013.
- [9] O. Barak and M. Tsodyks, "Working models of working memory," *Current Opinion in Neurobiology*, vol. 25, pp. 20–24, Apr. 2014.
- [10] Y. Burak and I. R. Fiete, "Fundamental limits on persistent activity in networks of noisy neurons," *Proceedings of the National Academy of Sciences*, vol. 109, pp. 17645–17650, Oct. 2012. PMID: 23047704.
- [11] Z. P. Kilpatrick, B. Ermentrout, and B. Doiron, "Optimizing working memory with heterogeneity of recurrent cortical excitation," *The Journal of Neuroscience*, vol. 33, no. 48, pp. 18999–19011, 2013.
- [12] K. Wimmer, D. Q. Nykamp, C. Constantinidis, and A. Compte, "Bump attractor dynamics in prefrontal cortex explains behavioral precision in spatial working memory," *Nature neuroscience*, vol. 17, no. 3, pp. 431–439, 2014.
- [13] P. M. Bays, "Noise in neural populations accounts for errors in working memory," *The Journal of Neuroscience*, vol. 34, no. 10, pp. 3632–3645, 2014.
- [14] A. Litwin-Kumar and B. Doiron, "Slow dynamics and high variability in balanced cortical networks with clustered connections," *Nature neuroscience*, vol. 15, no. 11, pp. 1498–1505, 2012.
- [15] R. Rosenbaum and B. Doiron, "Balanced networks of spiking neurons with spatially dependent recurrent connections," *Physical Review X*, vol. 4, no. 2, p. 021039, 2014.
- [16] M. Stern, H. Sompolinsky, and L. Abbott, "Dynamics of random neural networks with bistable units," *Physical Review E*, vol. 90, no. 6, p. 062710, 2014.
- [17] G. Mongillo, O. Barak, and M. Tsodyks, "Synaptic theory of working memory," *Science*, vol. 319, no. 5869, pp. 1543–1546, 2008.
- [18] D. Hansel and G. Mato, "Short-term plasticity explains irregular persistent activity in working memory tasks," *The Journal of Neuroscience*, vol. 33, pp. 133–149, Jan. 2013. PMID: 23283328.
- [19] S. Lim and M. S. Goldman, "Balanced cortical microcircuitry for maintaining information in working memory," *Nature Neuroscience*, vol. 16, pp. 1306–1314, Aug. 2013.
- [20] S. Lim and M. S. Goldman, "Balanced cortical microcircuitry for spatial working memory based on corrective feedback control," *The Journal of Neuroscience*, vol. 34, no. 20, pp. 6790–6806, 2014.
- [21] See Supplemental Material at [URL will be inserted by publisher] for additional details.
- [22] A. Renart, J. de la Rocha, P. Bartho, L. Hollender, N. Parga, A. Reyes, and K. D. Harris, "The asynchronous state in cortical circuits," *science*, vol. 327, no. 5965, pp. 587–590, 2010.